Herschel/PACS observations of the host galaxy of GRB 031203[★]

M. Symeonidis,[1,2][†] S. R. Oates,[2] M. de Pasquale,[2] M. J. Page,[2] K. Wiersema,[3] R. Starling,[3] P. Schady,[4] N. Seymour[5] and B. O'Halloran[6]

[1]*Astronomy Centre, Department of Physics and Astronomy, University of Sussex, Brighton BN1 9QH, UK*
[2]*Mullard Space Science Laboratory, University College London, Holmbury St Mary, Dorking, Surrey RH5 6NT, UK*
[3]*Department of Physics and Astronomy, University of Leicester, University Road, Leicester LE1 7RH, UK*
[4]*Max-Planck-Institut fr extraterrestrische Physik, Giessenbachstrasse, D-85748, Garching, Germany*
[5]*CSIRO Astronomy and Space Science, PO Box 76, Epping, NSW 1710, Australia*
[6]*Imperial College London, Astrophysics, Blackett Laboratory, Prince Consort Road, London SW7 2AZ, UK*

ABSTRACT

We present *Herschel*/PACS observations of the nearby ($z = 0.1055$) dwarf galaxy that has hosted the long gamma-ray burst (LGRB) 031203. Using the PACS data, we have been able to place constraints on the dust temperature, dust mass, total infrared (IR) luminosity and IR-derived star formation rate (SFR) for this object. We find that the GRB host galaxy (GRBH) 031203 has a total IR luminosity of 3×10^{10} L$_\odot$ placing it in the regime of the IR-luminous galaxy population. Its dust temperature and specific SFR are comparable to that of many high-redshift ($z = 0.3$–2.5) IR-detected GRB hosts ($T_{\rm dust} > 40$ K; sSFR > 10 Gyr^{-1}); however, its dust-to-stellar mass ratio is lower than what is commonly seen in IR-luminous galaxies. Our results suggest that GRBH 031203 is undergoing a strong starburst episode and its dust properties are different to those of local dwarf galaxies within the same metallicity and stellar mass range. Furthermore, our measurements place it in a distinct class to the well-studied nearby host of GRB 980425 ($z = 0.0085$), confirming the notion that GRB host galaxies can span a large range in properties even at similar cosmological epochs, making LGRBs an ideal tool in selecting samples of star-forming galaxies up to high redshift.

Key words: galaxies: dwarf – galaxies: general – galaxies: starburst – gamma-rays: general – infrared: general.

1 INTRODUCTION

The currently favoured scenario for the origin of long gamma-ray bursts (LGRBs) is that they result from the collapse of massive, metal-poor stars and as a result LGRBs are thought to mark the sites of cosmic star formation (e.g. Christensen, Hjorth & Gorosabel 2004; Tanvir et al. 2004). In comparison to the typical flux-limited galaxy surveys, LGRBs are considered more unbiased identifiers of star-forming galaxies (SFGs) because their occurrence and detection is independent of many galaxy properties, such as extinction (e.g. Ramirez-Ruiz, Trentham & Blain 2002; Watson et al. 2011). As a result, the follow up of LGRB hosts plays a key role in determining the cosmic star formation history and at high

redshift ($z > 5$) it has important implications for our understanding of the epoch of reionization (e.g Robertson & Ellis 2012).

Targeted observations of LGRB host galaxies have shown them to be young, spanning a large range of properties (e.g. Krühler et al. 2011; Perley et al. 2013); however, the role of dust in the star formation history, chemical enrichment and evolution of these sources is still largely unclear. Determining host galaxy properties, such as dust extinction, using the LGRB afterglows (e.g. Schady et al. 2007; Starling et al. 2007) target only line-of-sight conditions and hence may only be typical of the local environment around the GRB event rather than the host itself, particularly since there is evidence that measurements over small scales are not necessarily representative of global galaxy attributes (e.g. Padoan et al. 2006). Furthermore, as the abundance of dust in SFGs implies that they radiate a large fraction of their energy in the infrared (IR), star formation rates (SFRs) derived from optical observations cannot account for deeply dust-embedded star-forming regions and have to rely on uncertain extinction corrections. Examining the IR part of the spectral energy distribution (SED) is thus essential in order to determine the total energy budget and global SFR, as well as
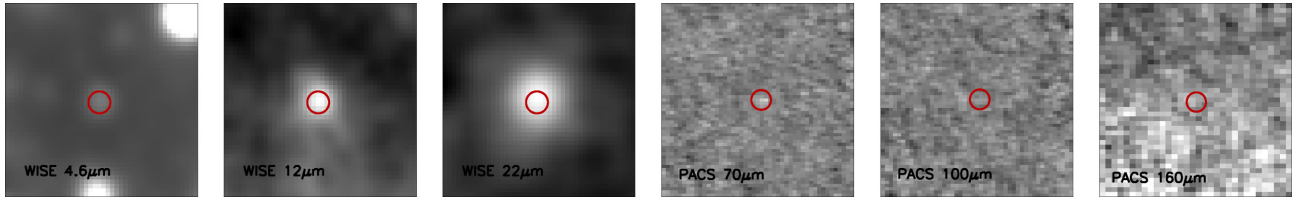
Figure 1. *WISE* and PACS images of GRBH 031203 (RA 08:02:30.18; Dec. −39:51:03.52). North is up and east is left. Each cut-out is 1 arcmin × 1 arcmin. The red circle denotes the position of the galaxy and has a radius of 6 arcsec.

dust properties such as temperature, mass and extinction. Indeed, estimating the gas-to-dust mass ratio, a key ingredient in constraining the chemical evolution of galaxies, is not feasible without IR observations. Ultimately, determining the role of dust in young environments, such as those found in LGRB host galaxies, is crucial for our understanding of primordial galaxy formation in the early Universe.

To date, out of the GRB host galaxies targeted in the IR with *Spitzer*/MIPS and JCMT/SCUBA, and more recently with *Herschel* (Hunt et al. 2014; Michałowski et al. 2014), only a small fraction have been detected (e.g. Tanvir et al. 2004; Le Floc'h et al. 2006; Michałowski et al. 2008). Here, we present *Herschel* (Pilbratt et al. 2010)/PACS (Poglitsch et al. 2010) observations of the host galaxy of GRB 031203 (hereafter referred to as GRBH 031203). GRBH 031203 is a metal-poor compact dwarf at $z = 0.1055$ (Prochaska et al. 2004; Margutti et al. 2007; Han et al. 2010; Levesque et al. 2010), one of the four local ($z \lesssim 0.1$) galaxies that have hosted a GRB event. Our aim is to place constraints on the dust properties and IR SED of this galaxy, which has not been possible to date due to lack of far-IR observations. This Letter is laid out as follows. Section 2 outlines the data used, Section 3 presents our SED measurements and in Section 4 we discuss the properties of GRBH 031203. Our summary and conclusions can be found in Section 5. Throughout we adopt a concordance cosmology of $H_0 = 70$ km s^{-1} Mpc^{-1}, $\Omega_M = 1 - \Omega_\Lambda = 0.3$.

2 DATA

2.1 *Herschel* data

We acquired *Herschel*/PACS 70, 100 and 160 μm data as part of the OT2 GO proposal cycle in 2013 (P.I. Symeonidis). Reduction of the PACS images was performed with the Herschel Interactive Processing Environment version 10.3.0.

From the PANIC *J*-band image in Gal-Yam et al. (2004), we see that GRBH 031203 is a compact source (∼2 arcsec). On the position of the host galaxy (see Fig. 1) we perform aperture photometry with the aperture photometry tool (APT[1]). We use an aperture radius of 12 arcsec and the prescribed aperture correction of 0.794 to determine the 70 μm flux density. For the 100 μm flux density, the same aperture size and an aperture correction of 0.766 is used, whereas for the 160 μm flux density, an aperture size of 22 arcsec and an aperture correction of 0.810 is used. To calculate 1σ photometric uncertainties and upper limits, we use the method outlined in the PACS documents (Muller et al. 2011; Balogh et al. 2013[2]). We check the validity of this method by calculating the standard

deviation of the distribution of flux densities measured in 20 same-sized apertures placed on empty parts of the map near the source. We find the 1σ deviation to be consistent with both methods. The PACS photometry is displayed in Table 1.

2.2 Multiwavelength data

We take optical photometry from Margutti et al. (2007) at $\lambda < 800$ nm, from Cobb et al. (2004) and Prochaska et al. (2004) at $\lambda < 3$ μm. We also use the *Spitzer* IRAC and MIPS 24 μm photometry from Watson et al. (2011). Watson et al. (2011) report that this source was also observed in the MIPS SED mode, which provides low-resolution spectroscopy between 52 and 100 μm, however, it was not detected and has an upper limit of 40 mJy. Our estimated flux density at 70 μm is consistent with this value. Finally, we also retrieve near- and mid-IR data from the *Wide-field Infrared Survey Explorer* survey (*WISE*; Wright et al. 2010) using the newly updated AllWISE Source Catalogue.[3] Table 1 shows the *WISE* photometry for GRBH 031203.

3 SED MEASUREMENTS

We fit the photometry of GRBH 031203, with a simple SED model, which combines the grey-body function (GBF) for the far-IR and a power law (PL) for the mid-IR at a critical frequency ν_* (see also Blain, Barnard & Chapman 2003; Younger et al. 2009) as follows:

$$F_\nu \propto \begin{cases} \frac{\nu^{3+\beta}}{e^{(h\nu/kT_{\rm dust})}-1} & \text{if } \nu < \nu_*, \\ \nu^\alpha & \text{if } \nu > \nu_*, \end{cases} \tag{1}$$

where F_ν is the flux density, h is the Planck constant, c is the speed of light in vacuum, k is the Boltzmann constant, $T_{\rm dust}$ is the temperature of the GBF and β is the emissivity – we adopt $\beta = 1.5$, consistent with studies of the far-IR emissivity of large grains (Desert, Boulanger & Puget 1990). At the critical frequency ν_*, the slopes of the two functions are equal and hence $\alpha = {\rm d} \log {\rm GBF}/{\rm d} \log \nu$. We perform χ^2 fitting to the dust component of the galaxy SED, i.e. from 4 μm onwards, in order to obtain the normalization, T and α. The 0.68 lower and upper confidence limits for our computed parameters resulting from the fits (e.g. temperature, total IR luminosity, etc.) are calculated according to the prescribed χ^2 confidence intervals for one interesting parameter, namely $\chi^2_{\rm min} + 1$, where $\chi^2_{\rm min}$ is the minimum χ^2. Fig. 2 shows the SED fit to the photometry.

We compute the total IR luminosity ($L_{\rm IR}$) in the 8–1000 μm range, $T_{\rm dust}$ (the average dust temperature of the galaxy representing the peak of the SED) and the dust mass ($M_{\rm dust}$) – see Table 2. $M_{\rm dust}$ is
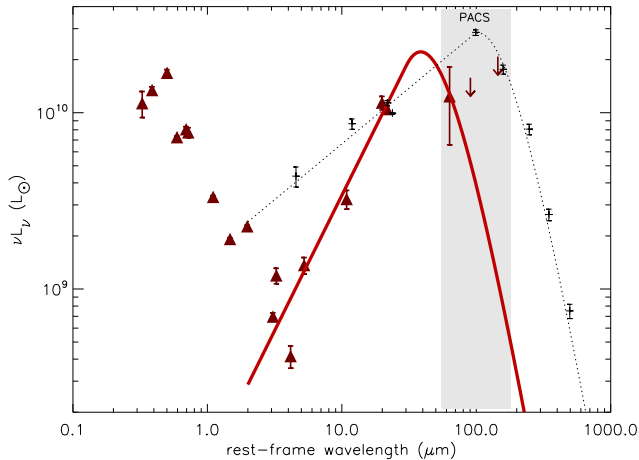
[1] http://www.aperturephotometry.org/
[2] http://herschel.esac.esa.int/twiki/bin/view/Public/PacsCalibrationWeb?template = viewprint

[3] http://wise2.ipac.caltech.edu/docs/release/allwise/

Table 1. The *WISE* (3.6, 5.4, 12 and 22 μm) and *Herschel* PACS (70, 100 and 160 μm) flux density measurements (and 1σ errors) in mJy. The 3σ upper limits for 100 and 160 μm are shown in parenthesis.

WISE 3.6 μm	*WISE* 5.4 μm	*WISE* 12 μm	*WISE* 22 μm	PACS 70 μm	PACS 100 μm	PACS 160 μm
0.11 ± 0.005	0.086 ± 0.009	1.74 ± 0.12	11.3 ± 1.0	39 ± 18	$22 \pm 16 \,(<70)$	$47 \pm 34 \,(<149)$

Figure 2. The SED of the GRBH 031203: photometry (red triangles and upper limits) and best-fitting SED model (red curve). For comparison, we overplot the SED of GRBH 980425 normalized at 20 μm to the SED of GRBH 031203 (dotted line: best fitting model; black points: photometry from M14).

Table 2. The derived properties from SED fitting, including upper and lower 1σ errors.

λ_{peak} (μm)	T_{dust} (K)	$\log L_{\mathrm{IR}}$ ($L_\odot$)	$\log M_{\mathrm{dust}}$ ($M_\odot$)	$\mathrm{SFR}_{\mathrm{IR}}$ ($M_\odot\,\mathrm{yr}^{-1}$)	$\mathrm{sSFR}_{\mathrm{IR}}$ (Gyr^{-1})
40^{+19}_{-8}	$68^{+13.3}_{-23.6}$	$10.47^{+0.006}_{-0.08}$	$4.27^{+0.7}_{-0.4}$	$5.06^{+0.07}_{-0.91}$	$20.2^{+3.6}_{-0.3}$

calculated as follows:

$$M_{\mathrm{dust}} = \frac{f_{\nu,\mathrm{rest}} D_{\mathrm{L}}^2}{B(\nu_{\mathrm{rest}}, T_{\mathrm{dust,rest}})\kappa_{\mathrm{rest}}}, \qquad (2)$$

where D_{L} is the luminosity distance, $B(\nu_{\mathrm{rest}}, T_{\mathrm{dust,rest}})$ is the blackbody function (in units of flux density), $f_{\nu,\mathrm{rest}} = \frac{f_{\nu,\mathrm{obs}}}{(1+z)}$, $\kappa_{\mathrm{rest}} = \kappa_{850\,\mu\mathrm{m}}(\frac{\nu_{\mathrm{rest}}}{\nu_{850\,\mu\mathrm{m}}})^{\beta}$ and $\kappa_{850\,\mu\mathrm{m}} = 0.0431$ m^2 kg^{-1} taken from Li & Draine (2001). Here, we take $f_{\nu,\mathrm{obs}}$ as the observed flux density at 250 μm computed by using the model SED and ν_{rest} is the rest-frame frequency equivalent to 250 μm (observed).

We convert L_{IR} to SFR using the prescription of Kennicutt (1998), finding $5.06^{+0.07}_{-0.91}$ M$_\odot$ yr^{-1} as the SFR of GRBH 031203. This is consistent with SFRs estimated from radio measurements: Stanway, Davies & Levan (2010) report an SFR of $4.8^{+1.4}_{-0.9}$ M$_\odot$ yr^{-1} and Michałowski et al. (2012) report an SFR of 3.83 ± 0.69 M$_\odot$ yr^{-1}. However, SFRs calculated from optical and UV measurements (mainly Hα and [O II] lines and UV continuum) are in disagreement varying from 0.4 to 13 M$_\odot$ yr^{-1} (Prochaska et al. 2004; Margutti et al 2007; Savaglio, Glazebrook & Le Borgne 2009; Levesque et al. 2010; Svensson et al. 2010; Guseva et al. 2011). It is likely that the discrepancies between the optical SFR measurements in literature are mainly due to discrepant extinction corrections. Stanway et al. (2010) also propose that optically derived SFR measurements for GRBH 031203 are subject to AGN contamination,

based on the conclusions of Levesque et al. (2010), however, many authors dispute the presence of an AGN (e.g. Prochaska et al. 2004; Margutti et al. 2007; Watson et al. 2011).

We calculate a specific SFR (sSFR) of 20.2 Gyr^{-1}, using the stellar mass of 2.5×10^8 M$_\odot$ reported in Guseva et al. (2011). The computed sSFR is within the range measured in other LGRB host galaxies (e.g. Castro Cerón et al. 2006; Savaglio et al. 2009; Perley et al. 2013).

Fig. 2 shows that the SED of GRBH 031203 is warm peaking at $\lambda_{\mathrm{peak}} = 40^{+19}_{-8}$ μm, consistent with a predisposition of low-metallicity SFGs to have SEDs which peak at short wavelengths (e.g. Galametz et al. 2009, 2011, 2013). For comparison, we overplot the SED of the nearest GRB host galaxy, GRBH 980425 ($z = 0.0085$), the only other local GRB host with *Herschel* observations. We fit the IR photometry reported in Michałowski et al. (2014) with the combination of grey-body/power-law functions as described earlier. It is interesting to note that GRBH 980425 has a cooler SED, which peaks at longer wavelengths ($\lambda_{\mathrm{peak}} = 104$ μm and $T_{\mathrm{dust}} = 25$ K).

Note that although GRBH 031203 is not significantly detected in the far-IR, the PACS data allow us to significantly constrain its IR SED shape and hence dust properties, particularly when combined with the mid-IR data from *WISE* and *Spitzer*/MIPS. In fact, even a simple visual inspection of the available photometry for GRBH 031203 in Fig. 2 indicates that the SED peak must be between 20 and 70 μm.

4 THE PROPERTIES OF GRBH 031203

In this section, we examine the dust properties of GRBH 031203 and compare to the following sources: (i) the *Herschel* dwarf galaxy sample (*H*DGS; Madden et al. 2013, hereafter Ma13 and Rémy-Ruyer et al. 2013, hereafter RR13), consisting of 48 dwarf galaxies at $z < 0.05$ and selected to span the largest range in SFR and metallicity for dwarf galaxies in the local Universe, (ii) GRBH 980425 (Michałowski et al. 2014; hereafter M14), the only other GRB host galaxy in the local Universe observed by *Herschel*, (iii) the three SCUBA-detected GRB hosts at $z \sim 1$ from Michałowski et al. (2008; hereafter M08) and (iv) the seven *Herschel*-detected GRB hosts at $0.3 < z < 2.5$ from Hunt et al. (2014; hereafter H14).

Fig. 3 shows the locus of the above samples on the IR-luminosity–dust temperature (L_{IR}–T_{dust}) plane; for reference, we also plot the 1σ bounds of the L_{IR}–T_{dust} relation from Symeonidis et al. (2013) representative of the $z < 2$ IR-luminous galaxy population. Note that GRBH 031203 has a warm dust temperature and an IR luminosity in the regime of IR-luminous galaxies ($L_{\mathrm{IR}} > 10^{10}$ L$_\odot$). Interestingly, within the 1σ uncertainty, its dust temperature is closer to the one typically seen in many of the high-redshift IR-detected M08 and H14 GRB hosts, than to the *H*DGS and GRBH 980425. Fig. 4 shows T_{dust} versus sSFR; dust temperature is seen to correlate better with sSFR than SFR in IR-luminous galaxies (e.g. Magnelli et al. 2014), suggesting that the intensity of star-forming activity, rather than its rate, has a direct effect on the average dust temperature. Again the locus of GRBH 031203 is within the parameter space probed by many of the high-redshift IR-detected GRB hosts.
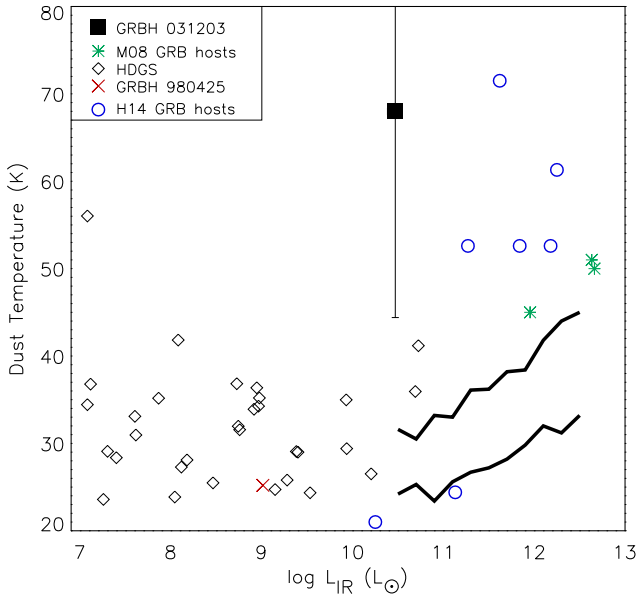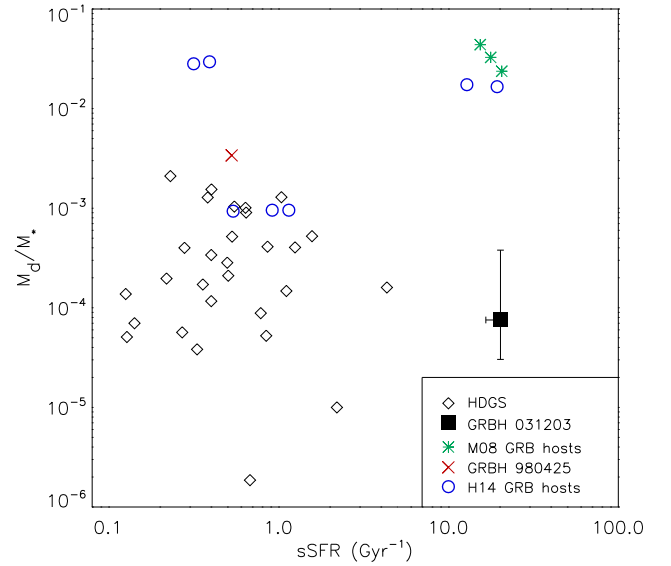
Figure 3. Dust temperature as a function of total IR luminosity. GRBH 031203 is denoted by a closed square. The diamonds are the *H*DGS from Ma13 and RR13 and the cross is GRBH 980425 from M14. The asterisks and open circles are the high-redshift IR-detected GRB hosts from M08 and H14, respectively. The lines are the 1σ bounds of the $L_{IR} - T_{dust}$ relation from Symeonidis et al. (2013) representative of the $z < 2$ IR-luminous galaxy population.
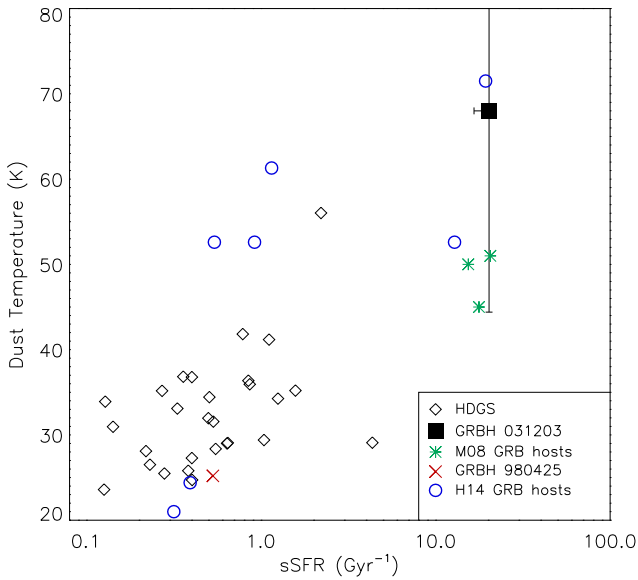
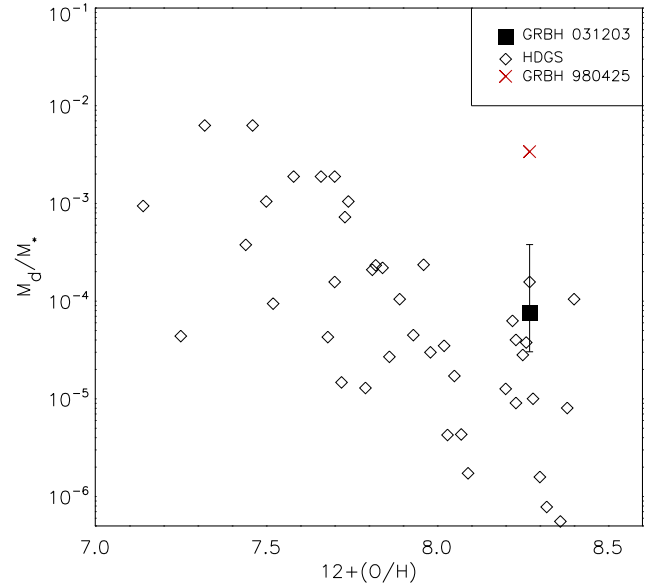**Figure 4.** Dust temperature as a function of sSFR. GRBH 031203 is denoted by a closed square. The diamonds are the *H*DGS from Ma13 and RR13 and the cross is GRBH 980425 from M14. The asterisks and open circles are the high-redshift IR-detected GRB hosts from M08 and H14, respectively.

In contrast, GRBH 980425 has a much smaller sSFR and a lower dust temperature.

Figs 5 and 6 show the dust-to-stellar mass ratio as a function of sSFR and metallicity, respectively. The *H*DGS spans a large range in dust-to-stellar mass ratio (M_d/M_*), however, all values lie at $\lesssim 0.002$, in agreement with normal SFGs locally (e.g. Skibba et al. 2011). This is in contrast to the high-redshift IR-detected GRB hosts whose values are higher, in the $0.001 < M_d/M_* < 0.1$

Figure 5. The dust-to-stellar mass ratio as a function of sSFR. GRBH 031203 is denoted by a closed square. The diamonds are the *H*DGS from Ma13 and RR13 and the cross is GRBH 980425 from M14. The asterisks and open circles are the high-redshift IR-detected GRB hosts from M08 and H14, respectively.

Figure 6. The dust-to-stellar mass ratio as a function of metallicity. GRBH 031203 is denoted by a closed square. The diamonds are the *H*DGS from Ma13 and RR13, the cross is GRBH 980425 from M14.

range, consistent with the general IR-luminous galaxy population (e.g. Santini et al. 2010). Interestingly, M_d/M_* for GRBH 031203 is well within the range of the *H*DGS, but significantly lower than GRBH 980425 and the $z \sim 1$ IR-detected GRB hosts.

5 SUMMARY AND CONCLUSIONS

We have reported *Herschel*/PACS observations of the host galaxy of GRB 031203. Using the PACS data and ancillary IR photometry, we have, for the first time, been able to place constraints on the IR SED shape, total IR luminosity, IR-derived SFR, dust mass and dust temperature of GRBH 031203. We compared our findings

with a representative sample of local dwarf galaxies, high-redshift IR-detected GRB hosts and the nearby well-studied GRB host 980425, the only other GRB host at $z < 0.1$ to have *Herschel* observations.

We found that GRBH 031203 has a warm average dust temperature, a high sSFR and an IR luminosity placing it in the regime of IR-luminous galaxies. Interestingly, these properties are comparable to those of the high-redshift IR-detected GRB host galaxies and unlike what is seen in local dwarfs. On the other hand, its value of M_d/M_* is within the range probed by local dwarf galaxies. GRBH 031203 is overall more active than typical local galaxies within the same metallicity and stellar mass range, consistent with previous reports of higher sSFR amongst GRB hosts compared to other SFGs (e.g. Castro Cerón et al. 2006; Savaglio et al. 2009; Perley et al. 2013). Its large sSFR indicates a starburst episode in action, in agreement with other studies of GRBH 031203 which conclude that it is a young system undergoing a starburst, the supporting evidence according to Watson et al. (2011) being the values of emission-line ratios (e.g. [Ne III]/[Ne II]), lack of polycyclic aromatic hydrocarbon features and a low value of the 4000 Å break ($D4000<1$).

Interestingly, GRBH 031203 is also in a separate class to the well-studied GRBH 980425. Although GRBH 031203 has similar metallicity to GRBH 980425, their T_{dust}, sSFR and M_d/M_* values are distinctly different. GRBH 031203 is a much more active system, whereas GRBH 980425 seems more quiescent, akin to local dwarfs. This is interesting because it suggests that GRB host galaxies can indeed span a large range in properties, making LGRBs an ideal tool in selecting relatively unbiased samples of SFGs up to high redshift ($z < 10$; e.g. Cucchiara et al. 2011).

REFERENCES

Blain A. W., Barnard V. E., Chapman S. C., 2003, MNRAS, 338, 733
Castro Cerón J. M., Michałowski M. J., Hjorth J., Watson D., Fynbo J. P. U., Gorosabel J., 2006, ApJ, 653, L85
Christensen L., Hjorth J., Gorosabel J., 2004, A&A, 425, 913
Cobb B. E., Bailyn C. D., van Dokkum P. G., Buxton M. M., Bloom J. S., 2004, ApJ, 608, L93
Cucchiara A. et al., 2011, ApJ, 736, 7
Desert F.-X., Boulanger F., Puget J. L., 1990, A&A, 237, 215
Gal-Yam A. et al., 2004, ApJ, 609, L59
Galametz M. et al., 2009, A&A, 508, 645
Galametz M., Madden S. C., Galliano F., Hony S., Bendo G. J., Sauvage M., 2011, A&A, 532, A56
Galametz M. et al., 2013, MNRAS, 431, 1956
Guseva N. G., Izotov Y. I., Fricke K. J., Henkel C., 2011, A&A, 534, A84
Han X. H., Hammer F., Liang Y. C., Flores H., Rodrigues M., Hou J. L., Wei J. Y., 2010, A&A, 514, A24
Hunt L. K. et al., 2014, A&A, 565, A112, (H14)
Kennicutt R. C., Jr, 1998, ARA&A, 36, 189
Krühler T. et al., 2011, A&A, 534, A108
Le Floc'h E., Charmandaris V., Forrest W. J., Mirabel I. F., Armus L., Devost D., 2006, ApJ, 642, 636
Levesque E. M., Berger E., Kewley L. J., Bagley M. M., 2010, AJ, 139, 694
Li A., Draine B. T., 2001, ApJ, 554, 778
Madden S. C. et al., 2013, PASP, 125, 600
Magnelli B. et al., 2014, A&A, 561, A86
Margutti R. et al., 2007, A&A, 474, 815
Michałowski M. J., Hjorth J., Castro Cerón J. M., Watson D., 2008, ApJ, 672, 817 (M08)
Michałowski M. J. et al., 2012, ApJ, 755, 85
Michałowski M. J. et al., 2014, A&A, 562, A70, (M14)
Padoan P., Cambrésy L., Juvela M., Kritsuk A., Langer W. D., Norman M. L., 2006, ApJ, 649, 807
Perley D. A. et al., 2013, ApJ, 778, 128
Pilbratt G. L. et al., 2010, A&A, 518, L1
Poglitsch A. et al., 2010, A&A, 518, L2
Prochaska J. X. et al., 2004, ApJ, 611, 200
Ramirez-Ruiz E., Trentham N., Blain A. W., 2002, MNRAS, 329, 465
Rémy-Ruyer A. et al., 2013, A&A, 557, A95
Robertson B. E., Ellis R. S., 2012, ApJ, 744, 95
Santini P. et al., 2010, A&A, 518, L154
Savaglio S., Glazebrook K., Le Borgne D., 2009, ApJ, 691, 182
Schady P. et al., 2007, MNRAS, 377, 273
Skibba R. A. et al., 2011, ApJ, 738, 89
Stanway E. R., Davies L. J. M., Levan A. J., 2010, MNRAS, 409, L74
Starling R. L. C., Wijers R. A. M. J., Wiersema K., Rol E., Curran P. A., Kouveliotou C., van der Horst A. J., Heemskerk M. H. M., 2007, ApJ, 661, 787
Svensson K. M., Levan A. J., Tanvir N. R., Fruchter A. S., Strolger L.-G., 2010, MNRAS, 405, 57
Symeonidis M. et al., 2013, MNRAS, 431, 2317
Tanvir N. R. et al., 2004, MNRAS, 352, 1073
Watson D. et al., 2011, ApJ, 741, 58
Wright E. L. et al., 2010, AJ, 140, 1868
Younger J. D. et al., 2009, MNRAS, 394, 1685

This paper has been typeset from a TEX/LATEX file prepared by the author.